coatings

MDPI

Article

An Experimental Study and Adaptability Evaluation of Chain Extender Component in Water Reducer on the Sulfate Corrosion Resistance of Ordinary Concrete

Bin Wu [1,*], Xianjun Li [1], Xianjie Meng [2], Yuanyaun Zhang [3], Lijun Zhao [1] and Qiang Zhang [1]

[1] School of Electric Power, Civil Engineering and Architecture, Shanxi University, Taiyuan 030031, China; 13835116998@163.com (X.L.); zhao186529@foxmail.com (L.Z.); zhangxq@sxu.edu.cn (Q.Z.)
[2] College of Civil Engineering, Taiyuan University of Technology, Taiyuan 030024, China; mengxianjie01@tyut.edu.cn
[3] China Special Equipment Testing and Research Institute, Beijing 100013, China; zhangyuanyuan@csei.org.cn
* Correspondence: wubin3515@sxu.edu.cn

Abstract: In Shanxi Province, China, concrete foundations of substations are widely exposed to environments with sulfate erosion, which results in severe damage. There are various avenues to enhance sulfate resistance, and one promising approach involves optimizing high-performance water reducers. Chain extender, which is an integral component of a water reducer, serves as a pore-blocking agent to effectively counter sulfate erosion. This study delves into the impact of a chain extender in the water reducer on the sulfate resistance and adaptability of ordinary concrete. The assessment begins with gauging the sensitivity of concrete to sulfate erosion, utilizing a 0–1 scoring method. Comparable conditions are maintained, allowing for a direct comparison between concrete with and without chain extender based on predefined criteria. A score of 1 denotes superior performance, while a score of 0 indicates a poorer performance. Following the evaluation of each criterion, scores are aggregated by the water reducer type, with higher scores signaling superior adaptability. The findings highlight that chain extender enhances the internal porosity of concrete, resulting in a more compact microstructure, heightened impermeability, and improved resistance to sulfate erosion. Its influence on mixture performance, however, is marginal. From an erosion product standpoint, using the semi-immersion method, chemical erosion predominates in the immersion zone, while both chemical and physical erosion are observed in the alternate wet–dry zone. Employing a 0–1 scoring method, Water Reducer 3# (with chain extender) scores 20 points, whereas Water Reducer 3#–1 (without chain extender) scores 4 points. Taking into consideration all factors, the chain extender demonstrates excellent adaptability to ordinary concrete. To validate the effectiveness of the 0–1 scoring method, it is applied to assess fly ash and slag double-blended concrete. Water Reducer 3# (with chain extender) scores 13 points, while Water Reducer 3#–1 (without chain extender) scores 10 points. Taking all aspects into consideration, the chain extender component exhibits commendable adaptability to fly ash and slag double-blended concrete.

Keywords: water reducer; chain extender component; sulfate resistance; concrete; adaptability; evaluation

Citation: Wu, B.; Li, X.; Meng, X.; Zhang, Y.; Zhao, L.; Zhang, Q. An Experimental Study and Adaptability Evaluation of Chain Extender Component in Water Reducer on the Sulfate Corrosion Resistance of Ordinary Concrete. *Coatings* **2023**, *13*, 1958. https://doi.org/10.3390/coatings13111958

Academic Editor: Edoardo Proverbio

Received: 14 October 2023
Revised: 7 November 2023
Accepted: 13 November 2023
Published: 16 November 2023

1. Introduction

At the forefront of safeguarding national security and fostering a sustainable, clean energy supply, the State Grid Corporation of China stands as a linchpin in the realm of energy and power. Its swift and efficient energy transmission holds a pivotal role in the broader energy supply ecosystem. Within this landscape, substations emerge as indispensable keystones by ensuring the seamless operation of the power grid. Among these substations, the concrete foundation stands as a linchpin that bridges the upper structure with the bedrock beneath, and thus exerts direct influence over the service lifespan of the entire edifice. However, in Shanxi, this crucial foundation faces the formidable

challenges of severe erosion and alkali–aggregate reactions, casting a shadow over both the longevity and aesthetic appeal of concrete structures. Figure 1 illustrates instances of alkali–aggregate reactions, concrete degradation, and surface spalling in the transitional zone of a substation's concrete foundation in Shanxi Province, China.

Figure 1. Corrosion failure diagram of the concrete foundation in a substation.

A project team has embarked on a meticulous chemical analysis of the lustrous white crystalline substance nestled within the transition zone of a substation's concrete foundation. The findings unveiled a dominant presence of Na_2SO_4 as its primary constituent [1]. Extensive investigations have illuminated the prevalence of sulfate-prone environments in Shanxi, resulting in the relentless onslaught of sulfate erosion upon these foundational structures [1]. Substation projects, which are monumental in their significance for national welfare and livelihoods, beckon the quest for solutions against erosive forces and the peculiar effects culminating in the specter of "concrete corrosion and alkali–aggregate reactions." The formulation of concrete that stands impervious to both sulfate and alkali effects and is tailored expressly for application in substation projects promises to bestow substantial economic and societal dividends.

In response to the deleterious impact of sulfate erosion on concrete, erudite scholars and experts have undertaken multifaceted research endeavors. Jiang Jianhua et al. [2] delved into experimental research and scrutinized the influence of varying groundwater static pressures and fly ash content on concrete subject to sulfate erosion. Their efforts culminated in an insightful assessment of erosion depth and mechanical performance indicators after a rigorous 60-day erosion period. Qiao Hongxia [3] ingeniously melded Fick's second law with the modified Davis equation and developed a numerical simulation process for ion diffusion of concrete within a sulfate-saturated immersion milieu, under the intricate interplay of myriad ions. This endeavor resulted in a streamlined model for sulfate immersion scenarios. Yan Changwang et al. [4] embarked on experimental research that meticulously examined the impact of steel fibers on concrete's fortitude against sulfate erosion. Their findings resoundingly underscored the enhancement of concrete's resistance to sulfate erosion through the incorporation of fibers. Hou Yingying [5], in turn, spearheaded experimental research that explored the augmentative influence of blended fibers on concrete's capacity to withstand sulfate erosion. The outcomes eloquently testified to a reduction in water absorption and the corresponding fortification of concrete's sulfate resistance. Zhang Hongliang et al. [6] astutely discerned that, during the drying phase, the corrosion and impairment of the concrete surface stem was predominantly due to the absorption of water by sodium sulfate, while deeper layer corrosion and damage could be traced to the annihilation of ettringite and gypsum. Li Hua et al. [7] harnessed microscopic testing techniques to probe sulfate erosion and ultimately revealed that the curtailment of C3A content in cement, the catalytic prowess of volcanic ash, and the replete effect of fine aggregate exerted a profoundly salutary impact on concrete's resistance to sulfate erosion. Niu Ditao et al. [8] postulated that the preeminent corrosion byproduct of concrete was ettringite. Wang Hailong et al. [9] adroitly employed scanning electron microscopy

to meticulously scrutinize the spatial disposition of ettringite and gypsum crystals within the sinews of pores and crevices. Finally, Yang Yonggan et al. [10] meticulously dissected concrete specimens bearing varying water-to-cement ratios and revealed a nuanced degradation mechanism. At high water-to-cement ratios, gypsum emerged as the chief agent of crystal erosion, while at lower ratios, the ascendancy of ettringite-induced erosion came to the forefront. Yang, W. et al. [11] found that substation construction exposed to stray current would accelerate concrete corrosion. Therefore, the effect of stray current on concrete corrosion was studied experimentally. The results showed that the damage degree of concrete was closely related to the corrosion of steel bar and the dissolution of calcium ions. Golewski, G. L. [12] reviewed the influence of fly ash (CFA) on water movement in concrete structures. It was found that 30% CFA concrete composites could improve the durability of reinforced concrete structures subjected to immersion conditions.

Zhu Miaomiao et al. [13] embarked on a pioneering venture and concocted high-strength concrete through the amalgamation of silica fume and Class II fly ash. The remarkable findings underscored the potency of silica fume and Class II fly ash in fortifying the sulfate resistance of high-strength concrete. In a study led by Geng Ou et al. [14], concrete specimens boasting a 50% replacement rate of recycled aggregate were subjected to an array of challenging environments including Na_2SO_4 solution, $MgSO_4$ solution, NaCl-Na_2SO_4 composite solution, and NaCl-$MgSO_4$ composite solution. Their meticulous inquiry revealed a compelling revelation, i.e., chloride ions could wield a formidable inhibitory effect on sodium sulfate erosion within recycled concrete.

The astute work of Wang Maosang et al. [15] ventured into a nuanced exploration of the chain extender component in four variants of polycarboxylic acid high-performance water reducers. Their discovery was nothing short of groundbreaking—the modified component demonstrated a remarkable augmentation in cement dispersion. In addition to ettringite, gypsum emerges as a pivotal player in the discourse on sulfate erosion, with its formation leading to the lamentable softening and spalling of concrete [16]. Esteemed scholars such as Santhanam [17], Neville [18], and Schmidt [19], to name a few, have posited that the erosion products are intimately entwined with the SO_4^{2-} concentration within the concrete's ambient milieu. At heightened concentrations, gypsum reigns supreme, while at more modest levels, ettringite takes the center stage. With the ascension of SO_4^{2-} concentration in the solution, the erosion products seamlessly transition from ettringite to gypsum. Meanwhile, luminaries like Liu [20] and Bellmann [21] have contended that sulfate erosion products bear a complex relationship not only with SO_4^{2-} concentration but also with the pH value of the solution. The groundbreaking insights of Xie Chao et al. [22] posited a tantalizing link between the resistance of cement-based composite cementitious materials to sulfate corrosion and temperature. A profound shift in corrosion mode and product manifestation occurred, with diminishing erosion temperatures heralding a crescendo in corrosion intensity. Meanwhile, the insightful analysis and research conducted by Zhang Meng [23] has illuminated the catalytic role of sulfate in fostering the proliferation of ettringite within concrete, ultimately leading to structural harm. Zhang Xinbo et al. [24] delved into the intricate interplay of water-to-cement ratio and sulfate corrosion resistance. Their revelations paint a clear picture, i.e., resistance to sulfate corrosion experiences a negative correlation with the water-to-cement ratio. Simply put, higher ratios spell lower resistance. To further deepen our understanding, some scholars have undertaken pioneering research and they have scrutinized the interplay of sulfate corrosion and other factors in shaping concrete's sulfate resistance [25–27].

In summary, the sulfate resistance of concrete has attracted significant attention from scholars and experts. It is widely believed that there are multiple possibilities to enhance sulfate resistance. On the one hand, synergistic effects between composite material components can be utilized [28–30], improving the concrete's microstructure. For instance, Wei H [30] conducted experiments on the compressive strength and sulfate resistance of slag-based geopolymer concrete with sodium chloride and gypsum. The results demonstrated that the combination of sodium chloride and gypsum exhibited a superimposed

effect, and the cross-reaction products had a synergistic effect on strength enhancement, effectively addressing the issue of insufficient strength. Additionally, both sodium chloride and gypsum could enhance the sulfate corrosion resistance of geopolymer concrete; when sodium chloride and gypsum were combined, the sulfate corrosion resistance coefficient increased by 73.4%. For instance, Dong, Y. [31] found that MSW incinerator foam had an active and microaggregate effect, which could effectively fill pores, optimized pore structure, and improved impermeability.

Simultaneously, the elevation of sulfate resistance has been masterfully orchestrated through the empowerment of high-performance water reducers [32–37]. Among these, the stalwart presence of polycarboxylic acid high-performance water reducers looms large, reigning supreme in the formulation of sulfate-resistant concrete. Renowned for their prodigious water-reducing prowess and other commendable attributes, they have earned their stripes in engineering applications [32–37]. However, the singular nature of the mother liquor of these water reducers sometimes imposes constraints on their application. Additionally, adaptability issues may occasionally arise in the interaction between cement concrete and polycarboxylic acid-based water reducers. Notably, scholars both at home and abroad have undertaken transformative research endeavors, leveraging physical and chemical means to modify these water reducers, yielding noteworthy outcomes. In the realm of innovation, Zhang Ming and fellow trailblazers [38] delved into the synthesis and performance of multi-branched polycarboxylic acid water reducers. Their experiments were heralded as a resounding success, with their water reducer demonstrating heightened adaptability to cement. Meanwhile, the ingenious work of Wu Wei [39] in fortifying the anchoring groups within the comb-like structure of polycarboxylic acid, coupled with strategic adjustments to the main chain, side chains, and anionic groups, proved to be transformative. The introduction of phosphoric acid functional groups dramatically elevated the molecule's affinity for cement particle surfaces, thereby amplifying the water reducer's adaptability. In a similar vein, the brainchild of Jiang Z [40] emerged as a vinyl polyoxyethylene ether-type polycarboxylic acid water reducer, i.e., PCE-6C. Synthesized through the artful copolymerization of vinyl polyoxyethylene ether and acrylic acid, its adaptability stood as a testament to the power of innovative chemistry. Zeyu Lin [41] embarked on a groundbreaking endeavor by harnessing HPEG and acrylic acid as primary raw materials and orchestrated redox reactions with catalysts like H_2O_2. This aqueous solution polymerization yielded a revolutionary high-performance HPEG-type polycarboxylic acid water reducer, aptly named PCE-A; the results were nothing short of astounding, showcasing PCE-A's remarkable ability to trim down additive dosage while elevating concrete strength. In a parallel quest for perfection, Song Zuobao et al. [42] undertook a meticulous exploration and scrutinized the influence of grafting density, main chain polymerization degree, and side chain length on polycarboxylic acid water reducers. Their endeavors culminated in a mathematical model that delineated the ideal molecular structure of PCE, a model that was triumphantly validated. Meanwhile, the ingenious work of Zhang Ming [43] resulted in the synthesis of a low air-entraining and shrinkage-reducing polycarboxylic acid water reducer, effectively putting an end to the specter of excessive concrete shrinkage. Similarly, Tan Liang [44] employed ether and olefin as polymerization monomers and launched a redox system with hydrogen peroxide. This brilliant orchestration yielded a highly versatile polycarboxylic acid water reducer, complete with an optimal synthesis process. Venturing into uncharted territories, Zhu Xiaofei et al. [45] harnessed ester ether in a polymerization endeavor and developed a copolymerized polycarboxylic acid water reducer; the results were nothing short of spectacular, showcasing the water reducer's prowess in heightening water reduction rates and overall strength. In tandem, Lai Huazhen [46] blazed a trail by employing vinyl ether monomers and introducing micro-crosslinking agents into the molecular structure, which resulted in a polycarboxylic acid water reducer that boasted superior adaptability to concrete. The terrain of adaptability between polycarboxylic acid water reducers and cement was the focal point for scholars like Guo Fei [47], who delved into a comprehensive investigation. Their findings illuminated the intricate relationships

between factors like grinding time, gypsum content, clinker source, and the performance of polycarboxylic acid water reducers in the realm of adaptability. The pioneering work of Tang Xiaobo et al. [48] in the realm of triethanolamine grinding aids created an elegant solution to the adaptability question. Their experiments unveiled excellent adaptability at dosages ranging from 0% to 0.02%. In a bid to consider all factors, Lu Cong [49] conducted a deep exploration of adaptability between polycarboxylic acid water reducers and a diverse array of cement types. The verdict was unanimous, i.e.,both ordinary Portland cement and Portland slag cement exhibited commendable adaptability. With a focus on the longevity of concrete, Tang Haibin [50] took center stage by pioneering a concrete corrosion-resistant additive. The results spoke volumes, affirming the additive's remarkable efficacy in fortifying concrete against sulfate erosion. Meanwhile, Cai Peng [51] left no stone unturned in refining polycarboxylic acid water reducers. Through the creation of a bespoke catalytic initiation system, adaptability and plasticizing performance were elevated to new heights. Su Jiang [52] synthesized two types of polycarboxylic acid water reducers with polyether side chains, and their adaptability to cement was studied.

Looking ahead, the trajectory of polycarboxylic acid water reducers appears to veer towards functionalization, greenification, and heightened performance. The initial hurdle to surmount lies in cement adaptability, a challenge that beckons innovation. Additionally, the intricate tapestry of concrete durability under sulfate erosion calls for meticulous refinement of results. The main focus of this study is the transformation of a high-performance polycarboxylic acid water reducer through the infusion of chain extender component. How does this adapted-water reducer fare in bolstering concrete's resistance to sulfate erosion? Starting with the study of the adaptability of the chain extender component to various properties of concrete, this paper presents a synthetic evaluation using a 0–1 scoring method. The results show that the chain extender component has excellent comprehensive properties and broad application prospects. At the same time, the research method can also provide some theoretical support and technical reference for durability design such as sulfate resistant concrete, and can benefit the sustainable development of cement industry and concrete industry.

2. Test

2.1. Raw Materials Overview

(1) Cement: The P·O42.5 was produced at the Shanxi Jigang Cement Co., Ltd. in Taiyuan City, Shanxi Province, China. Testing of the basic properties was conducted in accordance with established standards [53–55]. The results, as depicted in Table 1, affirm the basic properties of the cement.

(2) The sand was medium sand produced in Wenshui County, Shanxi Province. The performance index of the sand is shown in Table 2, and the sieve allowance of sand obtained using a screening test is shown in Table 3.

Table 1. Basic properties of the cement.

Specific Surface Area/m^2/kg	Setting Time/Min		3d Strength/MPa		28d Strength/MPa	
	Initial Setting	Final Setting	Flexural	Compression Resistance	Flexural	Compression Resistance
324	167	218	5.0	22.1	8.5	49.2

Table 2. Performance index of the sand.

Apparent Density/kg/m^3	Clay Content/%	Clay Lump Content/%	Alkali Activity (14 d Expansion Rate)/%	Firmness/%
2670	2.2	0.1	0.04	6

Table 3. Cumulative screen sieve of the sand.

Sieve Hole Size/mm		4.75	2.36	1.18	0.60	0.30	0.15	Chassis
Cumulative Screen Sieve/%	Experiment 1	9.0	20.2	34.1	62.3	78.6	97.8	99.8
	Experiment 2	8.7	19.8	34.4	60.8	80.6	98.1	98.7

The fineness modulus of the sand is 2.7, which belongs to medium sand and the grain size distribution qualifies it as zone II sand.

(3) The crushed stone was produced in Taiyuan City, Shanxi Province, China, with a particle size range of 5–25 mm. The performance index of the crushed stone is shown in Table 4, and the sieve allowance of the crushed stone is shown in Table 5.

(4) The water reducer was produced by Shanxi Shanda Hesheng New Materials Co., Ltd. in Taiyuan City, Shanxi Province, China. It includes two formulations of polycarboxylic acid high-performance water reducers, distinguished as Water Reducer 3 (with chain extender) and Water Reducer 3#–1 (without chain extender). The specific formulations are detailed in Table 6.

Table 4. Performance index of the crushed stone.

Apparent Density/kg/m^3	Clay Content/%	Clay Lump Content/%	Firmness/%	Crushing Index/%	Alkali Activity (14 d Expansion Rate)/%
2580	0.1	0.1	1	9.6	0.03

Table 5. Cumulative screen sieve of the crushed stone.

Sieve Hole Size/mm		26.5	19	16	9.5	4.75	2.36	Chassis
Cumulative Screen Sieve/%	Experiment 1	4.5	20.8	40.8	85.0	93.1	98.5	100
	Experiment 2	4.2	21.3	45.7	85.1	92.4	97.8	100

Table 6. Formulations of water reducer. Unit, kg/t.

Recipe No.	Polycarboxylic Acid	Gluconic Acid, Sodium Salt	Sodium Tripolyphosphate	Sodium Hexametaphosphate	Sodium Bicarbonate	Chain Extender	Sodium Dodecyl Sulfate	Water	Water Reducing Rate
3#	140	15	5	70	4	3	0.3	762.7	≥25%
3#–1	140	15	5	70	4	0	0.3	762.7	≥25%

Note: 3# is Water Reducer 3 (with chain extender), 3#–1 is Water Reducer 3#–1 (without chain extender).

The polycarboxylic acid mother liquor is an ether-type, acrylic polyether (APEG) with the chemical structure $CH_2 = CHCH_{20}$ $(CH_2CH_{20})_nH$. It is a light-yellow transparent liquid with a solid content of 40% and a density of 1.10 g/mL, and it is the main component of the admixture.

Gluconic acid, sodium salt is an organic compound with the chemical formula $C_6H_{11}NaO_7$ and molecular weight of 218.14. It is a white crystalline powder that is highly soluble in water, with a density of 1.763 g/cm^3. It functions as a retarding and water-reducing component in the concrete admixture.

Sodium tripolyphosphate (STPP) is an inorganic compound with the chemical formula $Na_5P_3O_{10}$ and molecular weight of 367.864. It is a white crystalline powder that readily dissolves in water, with a density of 2.52 g/cm^3. It is commonly used as a retarding and water-reducing component in concrete admixtures.

Sodium hexametaphosphate is an inorganic compound with the chemical formula $(NaPO_3)_6$ and molecular weight of 611.77. It is a white crystalline powder that easily dissolves in water, with a density of 2.181 g/cm^3. It functions as a slump-retaining component in the admixture.

Sodium bicarbonate is an inorganic compound with the chemical formula $NaHCO_3$ and molecular weight of 84.01. It is a white crystalline substance that readily dissolves in water, with a density of 2.20 g/cm^3. It serves as a component to block capillary pores in the admixture.

The chain extender was developed by the Shanxi Provincial Institute of Building Science in Taiyuan City, Shanxi Province, China. It is an organic amine, which is a derivative obtained by substituting hydrogen in NH_3 molecules with alkyl groups or similar. Its molecular formula is shown in Equation (1). The basic mechanism involves a polymerization reaction between the chain extender component and the water reducer, enhancing the dispersibility and slump retention of the water reducer [13]:

$$HX_1 - R_1 - NH - CO - O - R_2 - X_2H \quad (1)$$

where X_i (i = 1,2) represents NR or O (R is H or C1-6 alkyl), R_1 is $C_{1–20}$ alkyl, and R_2 is C_2 or C_3 alkyl or its isomer [15].

Sodium dodecyl sulfate (SDS) is an organic compound with the chemical formula $C_{12}H_{25}SO_4Na$ and a molecular weight of 288.379. It is a white powder that is easily soluble in water and serves as the air-entraining component in concrete admixtures.

(5) Fly ash is a Class II fly ash, produced by the Taiyuan Second Power Plant, with a fineness of 11%, water demand ratio of 101%, and moisture content of 0.2%.
(6) Slag was produced by the Shanxi Taiyuan Iron and Steel Group, with a specific surface area of 450 m^2/kg, a flowability ratio of 103%, and an ignition loss of 2.3%.
(7) The water was drinking water.
(8) Anhydrous sodium sulfate was used for preparing a 5% concentration Na_2SO_4 solution.

2.2. Test Research Method

2.2.1. Workability and Mechanical Properties of the Concrete Mixture

The mix proportions adhered to the specifications outlined in JGJ55-2011 [56] "Specification for Mix Proportion Design of Ordinary Concrete" and they are detailed in Table 7.

Table 7. Concrete mix proportions.

Numbering	Water Reducer	Strength Grade	W/B Ratio	Sand-Aggregate/%	Mix Proportion/kg/m^3				
					Cement	Sand	Gravel	Water	Water Reducer
C25-1-1	3#	C25	0.53	38	320	725	1185	170	6.4
C25-1-2	3#–1	C25	0.53	38	320	725	1185	170	6.4
C30-1-1	3#	C30	0.50	38	340	720	1170	170	6.8
C30-1-2	3#–1	C30	0.50	38	340	720	1170	170	6.8
C35-1-1	3#	C35	0.45	39	370	719	1126	167	7.4
C35-1-2	3#–1	C35	0.45	39	370	719	1126	167	7.4
C40-1-1	3#	C40	0.40	40	400	728	1092	160	8.0
C40-1-2	3#–1	C40	0.40	40	400	728	1092	160	8.0

Note: 3# is Water Reducer 3 (with chain extender), 3#–1 is Water Reducer 3#–1 (without chain extender). If C25-1-1 uses Water Reducer 3, C25-1-2 uses Water Reducer 3#–1, and so on.

The workability of the mixture was tested according to GB/T50080-2016 [57] "Standard for Test Methods of Performance on Ordinary Fresh Concrete". Two separate tests were conducted, with the average result being recorded.

The mechanical properties were tested according to GB/T50081-2019 [58] "Standard for test methods of physical and mechanical properties of concrete". The specimen size was 100 × 100 × 100 mm. For each mix proportion, two sets of specimens were prepared, with each set containing 3 pieces, totaling 6 pieces. The curing temperature was (20 ± 3) °C, with humidity levels maintained above 90%. Compressive strength was measured both at 7 and at 28 days.

2.2.2. Alkali Aggregate Reactivity of Concrete

In the quest to unravel the intricacies of alkali–aggregate reactions in concrete, samples of reaction products were meticulously gathered from concrete structures in Shanxi Province, China. The analysis revealed that a staggering 90% of these reaction products manifested as Na_2SO_4 [1]. In order to study the mechanism of concrete alkali flooding, the following experiments were carried out: A strategic immersion of the concrete in a 5% Na_2SO_4 solution was executed for a designated span. After extraction from the solution, the specimen's mass was meticulously measured, followed by a thorough drying process and another round of weighing. The discernible disparity in mass pre- and post-drying treatments shed light on the concrete's propensity to absorb the Na_2SO_4 solution. A substantial shift in mass signified an abundance of internal pores, hence heightened permeability. Conversely, a minimal shift indicated a scarcity of internal pores, translating to lower permeability. The methodology for gauging alkali–aggregate reaction products is expounded upon in Section 2.2.3.

The method for preparing the 5% Na_2SO_4 solution involved the following: Commence by ascertaining the total volume required for the solution. For illustration, let us consider 2000 milliliters (mL). Procure analytical-grade Na_2SO_4 and compute the requisite mass for a 5% Na_2SO_4 solution using the formula delineated in Equation (1). With the aid of an analytical balance, precisely measure out the Na_2SO_4 and dissolve it in a suitable vessel. Transfer the dissolved solution into a volumetric flask, then top up to 2000 mL with distilled water.

$$\frac{x}{2000\ \text{mL}} = \frac{5\ \text{g}}{100\ \text{mL}} \tag{2}$$

2.2.3. Sulfate Resistance of Concrete

The sulfate resistance of concrete is an amalgamation of internal permeability and surface characteristics. Therefore, a comprehensive evaluation of concrete's resistance to sulfate attack encompasses the following three vital aspects: a permeability test, a sulfate resistance test, and an alkali content test.

For the permeability test, according to GB/T50082-2009 [59] "Standard for test methods of long-term performance and durability of ordinary concrete", water pressure was incrementally applied to measure the permeability level. The specimens were cylindrical blocks with a diameter of 150 mm and a height of 150 mm. Each set of mix proportions produced 1 group with 6 blocks, and therefore a total of 6 blocks.

For the sulfate resistance test, following the guidelines of GB/T50082-2009 [60] "Standard for test methods of long-term performance and durability of ordinary concrete", cubic specimens with dimensions of 100 × 100 × 100 mm were used. Each set of mix proportions produced 2 groups with 3 blocks, totaling 6 blocks. The specimens were placed in a 5% Na_2SO_4 solution at 80 ± 5 °C for wet–dry cycles. The test was stopped when the erosion resistance coefficient reached 75% of the compressive strength or after 120 wet–dry cycles, whichever came first [60].

For the alkali content test, upon meticulous on-site observations, it was discerned that alkali efflorescence predominantly manifested near the juncture of soil and concrete. Consequently, the alkali content test employed a semi-immersion technique, which is illustrated in Figure 2. The internal alkali content finds indirect expression through the discernible shift in mass of the test blocks, while the external alkali content is deduced from the interaction of alkali efflorescence on the surface of the specimens. The precise experimental procedure involved cubic specimens exhibiting dimensions of 100 × 100 × 100 mm. Each formulation yielded a single group encompassing 3 blocks, aggregating to a total of 3 blocks. These specimens underwent semi-immersion in a 5% Na_2SO_4 solution. Following a stipulated number of wet–dry cycles, alkali efflorescence became evident. At three-day intervals, the efflorescence adorning the surface of the specimens was meticulously removed, weighed, and thus served as the external alkali content. For purposes of comparison, the alkali content on the surface of concrete specimens was measured at 15 days, 30 days, and 60 days using the semi-immersion method, offering insights into the concrete's resilience against

sulfate attack. The internal alkali content was acquired by scrupulously scraping off the alkali efflorescence from the specimens, weighing it, initiating the drying process, and subsequently reweighing it to ascertain the differential mass for each specimen.

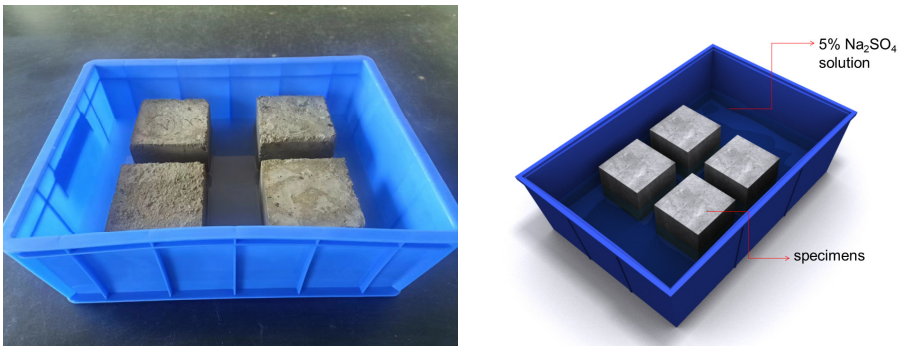

(**a**) (**b**)

Figure 2. Semi-immersion test chart of the 5% Na_2SO_4 solution. (**a**) Survey diagram of semi-immersion method. (**b**) Schematic diagram of semi-immersion method.

The genesis of alkali efflorescence primarily stems from the synergistic interplay of surface crystallization and internal infiltration within the concrete matrix. The semi-immersion methodology was deployed to assess the discernible mass shift of the concrete specimens and the attendant alkali content at the surface after 15 days, 30 days, and 60 days. A higher summation of the mass differential and surface alkali content, indicative of heightened alkali precipitation on the surface and a commensurate reduction in internal residue, augurs well for the concrete's fortitude against the sulfate onslaught. A segment of the experimental process is depicted in Figure 3.

Figure 3. Experimental process diagram.

2.2.4. Evaluation of the Adaptability of the Chain Extender Component to Concrete

The adaptability of the chain extender component to concrete is a comprehensive performance that is reflected not only in workability and strength but also in impermeability, sulfate erosion, and alkali efflorescence. It is imperative that while enhancing resistance to sulfate attack, the strength of concrete should not be significantly compromised. The evaluation of the adaptability between the chain extender component and concrete was mainly determined by comparing the properties, mechanical performance, and sulfate resistance of concrete mixtures with and without the chain extender component. This holistic approach considered the impact of the chain extender component on the adaptability of concrete.

The evaluation method employed a 0–1 scoring system. Under conditions where all other factors were equal, concrete mixtures containing the chain extender component were compared to those without the chain extender component. A score of 1 indicated better performance, while a score of 0 indicated poorer performance. For this evaluation, seven indicators were chosen, which included concrete slump loss, compressive strength

at 7 days, compressive strength at 28 days, compressive strength at 56 days, permeability grade, sulfate resistance grade, and alkali efflorescence. To simplify, it was assumed that each indicator carried equal importance. The judgment criteria which indicated better concrete performance were as follows: smaller slump loss, higher compressive strength, higher permeability grade, higher sulfate resistance grade, lower mass difference, and higher external alkali efflorescence. After scoring each indicator, a summary of scores was made based on the type of water reducer used. The higher the score, the better the adaptability was judged to be. The specific scoring rules are as follows.

For example, in the comparison of 7-day strength between C25-1-1 (with Water Reducer 3$^{\#}$) and C25-1-2 (with Water Reducer 3$^{\#}$–1), if C25-1-1 has higher compressive strength, then C25-1-1 receives 1 point and C25-1-2 receives 0 points. If C25-1-1 has lower strength, then C25-1-1 receives 0 points and C25-1-2 receives 1 point. If they are the same, since their scores do not affect the outcome, for simplicity, both receive 0 points, and so on.

The applicable scope of the evaluation method first involved summarizing which indexes affected performance; each selected index had an obvious comparable relationship and could be directly compared.

3. Results and Discussion

3.1. Workability and Mechanical Properties of the Concrete Mixtures

The test results are shown in Table 8 and Figure 4 below.

Table 8. Mix performances of mixtures.

Numbering	Slump/mm		Slump Loss/mm	Air Content/%	Initial Setting Time/min	Final Setting Time/min
	Initiation	1 h				
C25-1-1	220	195	25	2.0	341	472
C25-1-2	220	190	30	2.1	348	476
C30-1-1	220	190	30	2.1	345	470
C30-1-2	215	185	30	2.2	334	464
C35-1-1	225	190	35	2.2	328	462
C35-1-2	230	180	50	2.2	336	460
C40-1-1	215	190	25	2.3	343	474
C40-1-2	210	180	30	2.3	325	453

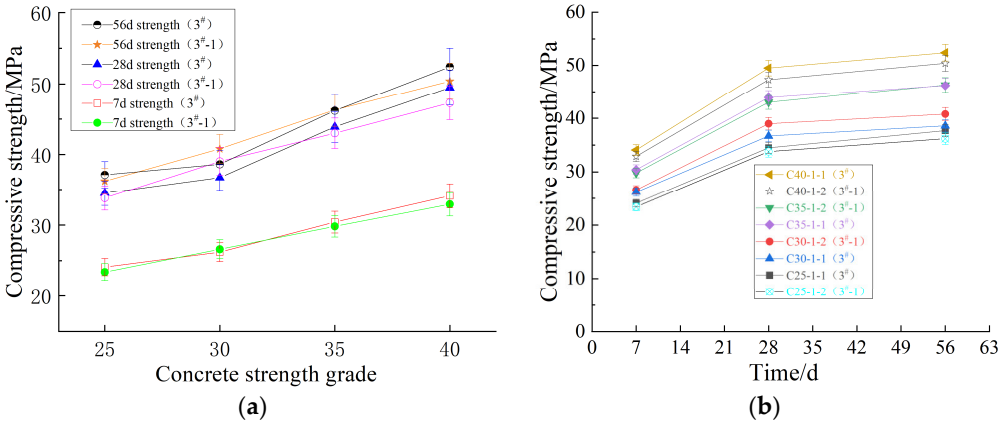

Figure 4. Compressive strength of ordinary concrete at different ages. (**a**) Compressive strength at concrete strength grade; (**b**) Compressive strength at different ages.

From Table 8 and Figure 4, the following conclusions can be made:

In terms of workability, concrete with the chain extender component exhibits an average slump loss of 28.8 mm compared to 35.0 mm for concrete without the chain extender component. This represents a substantial 21.5% reduction in slump loss. This improvement

can be attributed to the enhancing effect of the chain extender components on the internal pore structure, which in turn, leads to improved workability. Moreover, the air content in concrete with the chain extender component averages 2.15%, only slightly lower than the 2.20% observed in concrete without the chain extender component. This minor difference indicates that the chain extender has minimal impact on air entrainment. The initial and final setting times for concrete with the chain extender component were 339.25 min and 469.50 min, respectively. In contrast, for concrete without the chain extender component, the average initial and final setting times were 335.75 min and 463.25 min, respectively. These data demonstrate no significant difference in setting time, suggesting that the chain extender exerts only a slight influence in this regard. According to Wang Maosang [15], the modification mechanism of a chain extender essentially involves extending the length of side chains, increasing the quantity of short side chains, or enhancing the spatial hindrance effect of small molecules of the chain extender, thereby boosting the workability of concrete. Hamada D. [60] and Peng Xiongyi [61] posited that additives comprised of long-side chain water reducers and alternating long and short chains exerted a more potent dispersing effect on concrete.

In terms of mechanical properties, as concrete ages, its strength experiences a gradual, proportional increase. Overall, with the exception of the C30 concrete group, the concrete with the chain extender component exhibits higher strength compared to concrete without the chain extender component. This is likely attributed to the chain extender component's positive influence on the pore structure of the concrete, leading to increased density and subsequently enhanced strength.

3.2. Sulfate Resistance of Concrete

The results are shown in Table 9 and Figure 5.

Table 9. Test table for the sulfate resistance of concrete.

Numbering	Impervious Grade	Sulfate Resistance Rating	Sulphate Precipitation/g				Mass Difference/g
			15d	30d	60d	Σ60d	
C25-1-1	P8	KS30	10.04	8.11	6.71	24.86	5.85
C25-1-2	P7	KS30	7.36	6.23	5.17	18.76	9.78
C30-1-1	P9	KS60	17.91	14.23	11.02	43.16	7.53
C30-1-2	P8	KS30	8.23	7.56	5.85	21.64	10.52
C35-1-1	P10	KS60	19.00	16.42	12.53	47.95	7.64
C35-1-2	P10	KS30	9.08	8.77	6.32	24.17	14.53
C40-1-1	P11	KS60	19.70	16.81	12.81	49.32	6.55
C40-1-2	P11	KS30	10.85	10.22	8.77	29.84	14.59

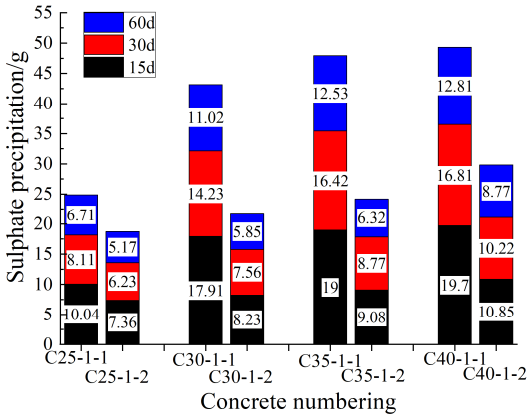

Figure 5. Sulphate precipitation of ordinary concrete.

From Table 9 and Figure 5, the following observations can be made:

In terms of permeability resistance, concrete specimens with the chain extender component (C25 and C30) exhibit one grade higher resistance compared to concrete without the chain extender component. Regarding sulfate resistance, concrete specimens with the chain extender component (C30, C35, and C40) show one grade higher resistance to sulfate erosion compared to the concrete without the chain extender component.

Regarding efflorescence, the average mass difference for specimens with the chain extender component is 6.89 g, while for specimens without the chain extender component, it is 12.36 g. The mass difference in specimens with the chain extender component is 44.3% lower compared to specimens without the chain extender component. This indicates that there is less internal adsorption of sulfates, suggesting a denser structure, which aligns with the findings from the permeability tests. Additionally, the amount of sulfate precipitation reveals that the total efflorescence on the surface of concrete specimens with the chain extender component, at 60 days, is 165.29 g, whereas for concrete specimens without chain extender component, it is 94.41 g. The total efflorescence on the surface of concrete specimens with the chain extender component is 75.08% lower compared to the concrete specimens without chain extender component. This indicates that the efflorescence on the surface of concrete specimens with the chain extender component is significantly higher than that without the chain extender component. This is mainly attributed to the fact that the chain extender component improves the internal pore structure of the concrete, making it denser. Consequently, sulfate ions in the solution have a harder time entering the pores, resulting in greater precipitation at the interface between wet and dry conditions. This leads to an improvement in the sulfate resistance of the concrete.

Overall, concrete specimens with the chain extender component exhibit better sulfate resistance compared to the concrete specimens without the chain extender component.

3.3. SEM Microscopic Analysis of Concrete

After curing under standard conditions for 56 days, the crushed areas of the specimens were reduced to particles measuring 2–3 mm. Then, the surfaces were coated with gold and observed under a scanning electron microscope (SEM) to examine the hydration products and pore structure. SEM images of the C25-1-1 and C25-1-2 specimens after 56 days of standard curing are shown in Figure 6.

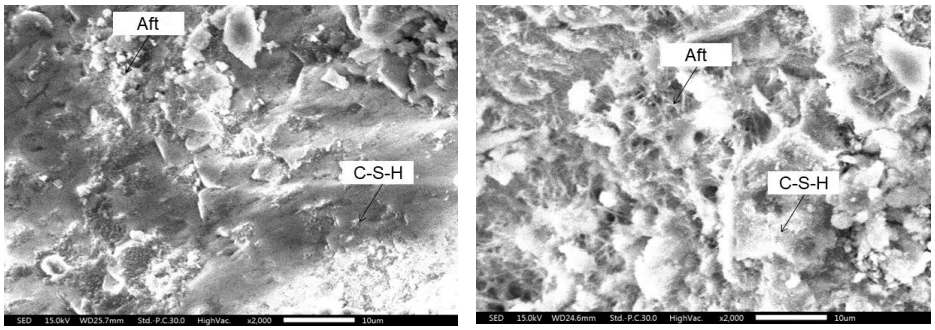

(**a**) (**b**)

Figure 6. SEM diagram: (**a**) C25-1-1 SEM diagram (×2500); (**b**) C25-1-2 SEM diagram (×2500).

Upon comparative observation, the following conclusions were drawn: The C25-1-1 and C25-1-2 specimens both exhibit a certain amount of C-S-H gel. On the one hand, C25-1-1 displays a well-defined reticular structure with fewer pores, indicating a denser microstructure. On the other hand, in C25-1-2, there are primarily gel-like hydration products, with noticeable amounts of ettringite. There are relatively more pores in C25-1-2, and its macroscopic performance is weaker compared to C25-1-1. This may be attributed to a polymerization reaction occurring between the chain extender and the polycarboxylate superplasticizer, resulting in an extension of the original chain length and the addition of some short chains. These short and long chains alternate, intertwining in a spatial structure. Furthermore, the organic amine molecules from the chain extender are dispersed between

the main and side chains, filling the gaps between the side chains and improving spatial steric hindrance. This leads to a denser microstructure in the concrete. Additionally, the unreacted organic amine molecules can accelerate cement hydration, enhancing concrete compactness. This phenomenon may also explain the characteristics of the concrete with the chain extender component, including its higher strength, greater efflorescence, improved workability, and enhanced permeability resistance.

3.4. Concrete Specimen Semi-Immersion and XRD Test Failure Mechanism

In general, sulfate attack on concrete is primarily caused by the reaction between SO_4^{2-} ions and the hydration products of cement inside the concrete. However, due to variations in the concentration of the erosive medium and the content of internal components of the concrete, the resulting products and reaction phenomena may differ. In practical engineering, sulfate-induced damage to concrete mainly takes three forms, i.e., self-absorption and expansion, ettringite destruction, and gypsum damage.

To investigate the failure mechanism of semi-immersed concrete specimens, a SEM analysis was performed on the immersion zone and the alternate wet–dry zone of the concrete specimens. The SEM images of the immersion zone and the alternate wet–dry zone are shown in Figure 7.

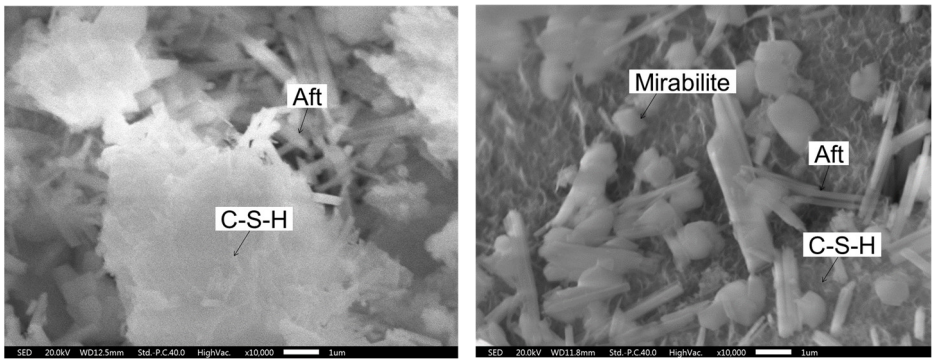

(**a**) (**b**)

Figure 7. SEM diagram of immersion zone and alternate wet–dry zone: (**a**) Immersion zone (×10,000); (**b**) Alternate wet–dry zone (×10,000).

From Figure 7, it can be observed that in the immersion zone, except for the presence of some ettringite, the other areas maintain good compactness. In the alternate wet–dry zone, there is a fibrous accumulation of ettringite in the cement, along with irregularly enlarged gypsum crystals. The gypsum is likely a reaction product of $Ca(OH)_2$ and sodium sulfate. Additionally, crystals of mirabilite ($Na_2SO_4{\cdot}10H_2O$) can be seen. These erosion products often lead to volume expansion during formation, causing the C-S-H gel to become looser and microcracks to form. Once cracks appear, the solution is more prone to infiltration, making it easier for crystals to precipitate, creating a vicious cycle. In the alternate wet–dry zone, there are also ettringite crystals in the cement, but their content is minimal. Chen et al. [62] suggested that for Na_2SO_4 semi-immersion specimens the immersion zone is only subjected to chemical erosion, while the alternate wet–dry zone is simultaneously subjected to both chemical and physical corrosion.

As shown in the above figures, the diffraction peaks corresponding to gypsum ($CaSO_4{\cdot}2H_2O$) and ettringite (Aft) in the spectrum of the alternate wet–dry zone are higher than those in the immersion zone, indicating that there are more corrosion products in the alternate wet–dry zone. Additionally, there is a certain height of mirabilite corresponding to the alternate wet–dry zone, indicating that chemical corrosion occurs simultaneously with physical corrosion in this area. The XRD images of the immersion zone and the alternate wet–dry zone are shown in Figure 8.

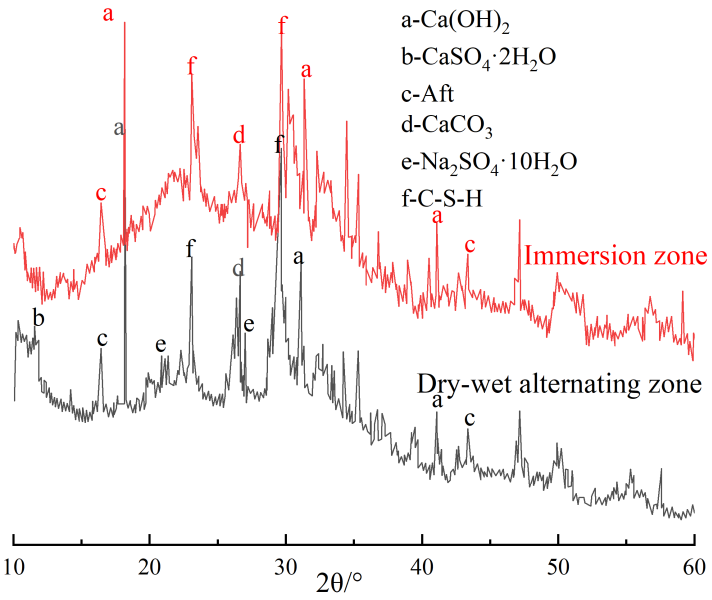

Figure 8. XRD diagram of immersion zone and alternate wet–dry zone.

Based on the above observations, it is believed that the concrete products in the immersion zone consist of hardened cement paste C-S-H and ettringite. This indicates that chemical erosion primarily occurs in this area. In the alternate wet–dry zone, in addition to the hardened cement paste C-S-H and ettringite generated from chemical reactions, there is also gypsum and mirabilite ($Na_2SO_4 \cdot 10H_2O$) primarily formed through physical crystallization. This suggests that this area is the result of the combined action of chemical and physical erosion, with gypsum being the predominant form of damage.

The process of sulfate corrosion can be divided into the following three stages [22,63]: (1) During the sulfate solution penetration stage, sulfate ions from the solution mainly permeate into the interior of the concrete. (2) During the erosion product generation stage, sulfate ions react chemically with the hydration products of the concrete, resulting in the formation of substances like ettringite and gypsum. These substances exhibit a certain degree of expansion [21,64,65]. (3) During the destruction stage, with the progression of wet–dry cycles, pores expand, and sulfate solution gradually infiltrates the concrete. It accumulates continuously within the pores. When the expansive materials generated in Stage 2, along with sulfate crystals, exceed the volume the pores can accommodate, they exert expansive stress. When this stress surpasses the ultimate stress of the pore walls, the pores crack, allowing more corrosive solution to enter the interior of the concrete. This process is repeated, generating more and larger cracks, eventually leading to complete penetration and ultimate failure.

3.5. Study on the Adaptability of the Chain Extender Component to Ordinary Concrete

Combining Tables 8 and 9 and Figures 4 and 5, scoring is conducted according to the evaluation criteria in Section 2.2.4. The adaptability assessment scores of the water reducer to ordinary concrete are shown in Table 10, with the alkali content indicator compared in terms of the cumulative value within 60 days.

Table 10. Evaluation score table of adaptability of water reducer to concrete.

Type of Water Reducer	Slump Loss Value	P	KS	Pan Alkali	Compressive Strength			Total Score
					7d	28d	56d	
3#	3	2	3	4	3	3	2	20
3#–1	0	0	0	0	1	1	2	4

Note: 3# is Water Reducer 3 (with chain extender), 3#–1 is Water Reducer 3#–1 (without chain extender).

As shown in Table 10, using the above evaluation method, Water Reducer 3 scores 20 points, while Water Reducer 3#–1 scores 4 points. Both types have similar scores in terms of compressive strength at 56 days. Water Reducer 3#–1 performs better in terms of alkali content, while Water Reducer 3# excels in other aspects. Taking all factors into consideration, the adaptability of the chain extender component to ordinary concrete is better. The adaptability of the water reducer to concrete is a comprehensive indicator. This evaluation method takes into consideration various aspects, including the workability and fluidity of the concrete mixture, concrete strength, impermeability, resistance to sulfate corrosion, alkali content, and other properties. It provides a comprehensive assessment of the adaptability of the water reducer to concrete and serves as a reference for further evaluating its suitability for concrete.

4. Evaluation Method Validity Verification

To validate the effectiveness of the evaluation method described above, the method was applied to concrete with fly ash and slag as dual admixtures, and the adaptability of the chain extender was compared and evaluated.

4.1. Mix Proportions of Concrete with Fly Ash and Slag as Dual Admixtures

The mix proportions are shown in Table 11 below.

Table 11. Mix ratio of concrete with fly ash and slag as dual admixtures.

Numbering	Water Reducer	Strength Grade	W/B Ratio	Sand-Aggregate/%	Mix Proportion/kg/m^3						
					Cement	Fly Ash	Slag	Sand	Gravel	Water	Water Reducer
C25-2-1	3#	C25	0.50	43	260	70	40	793	1052	185	7.4
C25-2-2	3#–1	C25	0.50	43	260	70	40	793	1052	185	7.4
C30-2-1	3#	C30	0.45	42	290	70	30	770	1063	176	7.8
C30-2-2	3#–1	C30	0.45	42	290	70	30	770	1063	176	7.8
C35-2-1	3#	C35	0.42	41	320	60	30	743	1069	172	8.2
C35-2-2	3#–1	C35	0.42	41	320	60	30	743	1069	172	8.2
C40-2-1	3#	C40	0.38	40	350	60	30	710	1066	167	8.8
C40-2-2	3#–1	C40	0.38	40	350	60	30	710	1066	167	8.8

Note: 3# is Water Reducer 3 (with chain extender), 3#–1 is Water Reducer 3#–1 (without chain extender). If C25-2-1 uses Water Reducer 3, C25-2-2 uses Water Reducer 3#–1, and so on.

4.2. Mix Performance and Mechanical Properties of Concrete with Fly Ash and Slag as Dual Admixtures

The test results are shown in Table 12 and Figure 9.

Table 12. Mix performance of concrete with fly ash and slag as dual admixtures.

Numbering	Slump/mm		Slump Loss/mm	Air Content/%	Initial Setting Time/min	Final Setting Time/min
	Initiation	1 h				
C25-2-1	235	200	35	2.3	365	490
C25-2-2	230	190	40	2.1	380	495
C30-2-1	220	205	15	2.1	348	478
C30-2-2	210	195	25	2.3	371	474
C35-2-1	225	195	30	2.5	355	487
C35-2-2	225	190	35	2.4	359	500
C40-2-1	205	190	15	2.6	300	474
C40-2-2	210	180	30	2.1	320	493

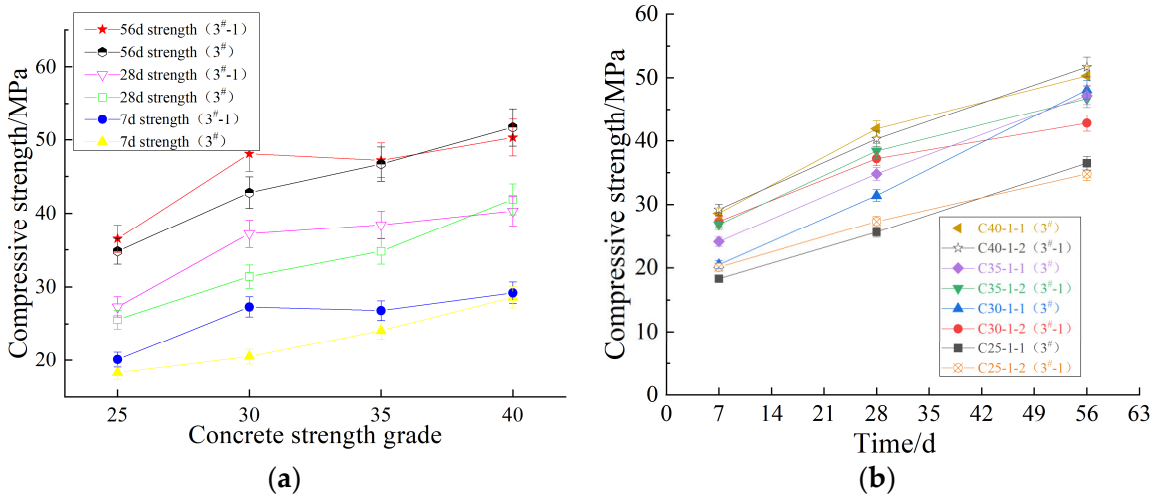

Figure 9. Compressive strength of concrete with fly ash and slag dual admixtures at different ages. (**a**) Compressive strength at concrete strength grade; (**b**) Compressive strength at different ages.

From Table 12 and Figure 9, the following observations can be made:

In terms of mixture performance, the average slump loss of concrete with the chain extender component is 23.75 mm, while that without the chain extender component is 32.50 mm. Compared to concrete without the chain extender component, the slump loss of concrete with the chain extender component is reduced by 26.9%. This indicates that the chain extender component can reduce the slump loss of concrete. This is likely due to the improvement in internal pore structure and workability enhancement brought about by the chain extender component.

The air content in concrete with the chain extender component averages 2.38%, whereas in concrete without the chain extender component, it averages 2.23%. With the chain extender component, the air content in concrete increases by 6.7%. This may be due to a reaction occurring between the chain extender and the admixture, resulting in an increased number of bubbles, thus leading to an increase in air content within the concrete.

Compared to regular concrete, the workability of concrete with the chain extender component in dual admixture concrete is significantly improved, indicating that the simultaneous use of chain extenders and admixtures helps to enhance the flowability of concrete.

Regarding setting time, the initial and final setting times for concrete with the chain extender component average 342.00 min and 482.25 min, respectively. For concrete without the chain extender component, the initial and final setting times average 357.50 min and 490.50 min, respectively. It can be observed that there is no significant difference in setting time, indicating that the impact of chain extenders on setting time is minimal.

In terms of mechanical performance, for lower strength grades of concrete with the chain extender component (C25, C30, and C35), the compressive strength is lower. However, for the higher strength C40 concrete, the late-stage strength of concrete with the chain extender component is even higher than that without the chain extender component. The early-stage strength growth of concrete with the chain extender component is slower, but the late-stage strength growth is faster. This may be due to two reasons: Firstly, the secondary hydration products of admixtures fill some of the pores, making the microstructure denser, thereby strengthening the concrete; secondly, after the cementitious material has set and hardened, the chain extender component reacts comprehensively with the admixtures, generating a certain colloidal substance, which increases the compactness of the concrete and enhances its strength.

In summary, regarding the adaptability of concrete with chain extender component to dual admixtures, the early-stage adaptability is weaker, while the late-stage adaptability is stronger.

4.3. Sulfate Resistance of Concrete with Fly Ash and Slag as Dual Admixtures

The results are shown in Table 13 and Figure 10.

Table 13. Test table for sulfate resistance of concrete with fly ash and slag dual admixtures.

Numbering	Impervious Grade	Sulfate Resistance Rating	Sulphate Precipitation/g				Mass Difference/g
			15d	30d	60d	Σ60d	
C25-2-1	8	60	9.52	8.01	6.52	24.05	4.98
C25-2-2	8	60	8.84	7.64	5.82	22.30	7.60
C30-2-1	9	90	10.11	8.23	6.31	24.65	7.08
C30-2-2	8	90	9.8	8.07	6.28	24.15	5.77
C35-2-1	11	90	10.09	8.46	6.82	25.37	8.73
C35-2-2	10	90	9.95	8.16	6.12	24.23	9.39
C40-2-1	12	90	10.07	9.02	6.33	25.42	12.78
C25-2-1	8	60	9.52	8.01	6.52	24.05	4.98

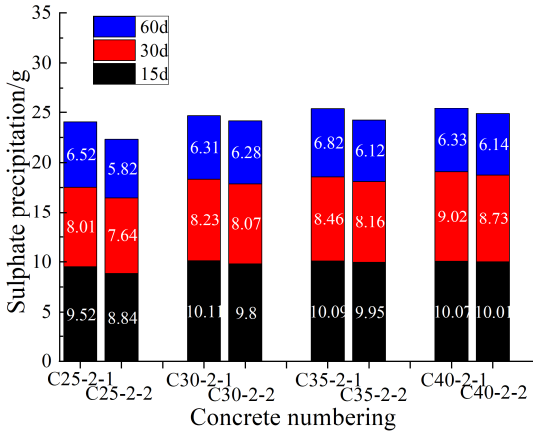

Figure 10. Sulphate precipitation of concrete with fly ash and slag as dual admixtures.

From Table 13 and Figure 10, the following observations can be made:

In terms of impermeability, concrete with the chain extender component in C25 and C30 exhibit a one-grade higher impermeability compared to concrete without the chain extender component. In terms of resistance to sulfate erosion, concrete with the chain extender component in grades C30, C35, and C40 demonstrate a one-grade higher resistance to sulfate erosion compared to concrete without the chain extender component.

Regarding efflorescence, from the mass difference, it can be seen that the average mass difference of specimens with the chain extender component is 8.39 g, while that without the chain extender component is 8.67 g. The mass difference in specimens with the chain extender component is reduced by 3.23% compared to those without the chain extender component. This indicates that there is less internal adsorption of sulfate, which also suggests a more compact structure, consistent with the conclusions from the permeability testing. Furthermore, looking at the amount of sulfate precipitation, the total efflorescence on the surface of concrete with the chain extender component at 60 days is 99.49 g, while that without the chain extender component is 95.56 g. The efflorescence on the surface of concrete with the chain extender component is reduced by 0.07% compared to that without the chain extender component. Overall, the efflorescence on the surface of concrete with the chain extender component is slightly lower than that without the chain extender component. This may be attributed to a reaction occurring between the chain extender component and the admixtures, which improves the internal pore structure of the concrete, making it denser. As a result, sulfate ions in the solution find it more difficult to enter the pores, leading to a higher precipitation at the wet–dry interface, enhancing the concrete's resistance to sulfate erosion.

In summary, concrete with the chain extender component in dual admixtures exhibits better resistance to sulfate erosion compared to concrete without the chain extender component.

4.4. Adaptability Evaluation of the Chain Extender Component to Concrete with Fly Ash and Slag as Dual Admixtures

Combining the information from Tables 12 and 13, as well as Figures 9 and 10, and following the scoring criteria in Section 2.2.4, the adaptability evaluation scores of the superplasticizer to concrete with fly ash and slag as dual admixtures are presented in Table 14. The efflorescence index is compared based on the cumulative value within 60 days (Σ60d).

Table 14. Evaluation score table of adaptability of water reducer to concrete with fly ash and slag as dual admixtures.

Type of Water Reducer	Slump Loss Value	P	KS	Pan Alkali	Compressive Strength			Total Score
					7d	28d	56d	
$3^{\#}$	4	3	0	4	0	1	1	13
$3^{\#}$–1	0	0	0	0	4	3	3	10

Note: $3^{\#}$ is Water Reducer 3 (with chain extender), $3^{\#}$–1 is Water Reducer $3^{\#}$–1 (without chain extender).

Based on Table 14, using the aforementioned evaluation method, Water Reducer 3 received a score of 13, while Water Reducer $3^{\#}$–1 received a score of 10. Each of them has its own advantages. Water Reducer 3 performs better in terms of impermeability, resistance to sulfate attack, and efflorescence, whereas Water Reducer $3^{\#}$–1 excels in terms of strength. Taking all factors into consideration, when formulating concrete with resistance to sulfate attack, Water Reducer 3 demonstrates better adaptability to concrete containing fly ash and slag as dual admixtures. Therefore, employing this evaluation method allows for a comprehensive assessment of the adaptability of superplasticizers to concrete.

Regarding the reasonableness of the evaluation method, the method is mainly used to evaluate the adaptability of the chain extender component to sulfate resistance concrete. The adaptability of concrete, reflecting not only in workability of concrete mix, strength after hardening, but also in impermeability, sulfate corrosion resistance, pan-alkali, etc., is a comprehensive performance. Using this method, the properties of concrete with and without the chain extender component can be graded and summarized. Concrete with a high score reflects good adaptability, otherwise, its adaptability is poor.

5. Conclusions

The adaptability of a chain extender component to resist sulfate attack in concrete is a comprehensive performance that is reflected not only in workability and strength but also in impermeability, sulfate attack resistance, and alkali–aggregate reactions. In order to study the adaptability of the chain extender component to ordinary concrete, an evaluation was conducted based on the sensitivity of various properties of concrete to the chain extender component using a 0–1 scoring method. The following conclusions were drawn:

(1) Through the SEM analysis, it was evident that the internal pores in concrete were significantly reduced by the chain extender component. The chain extender component improved the internal porosity of the concrete, resulting in a denser microstructure. As a result, the concrete's impermeability and sulfate corrosion resistance was enhanced, while the impact on the properties of the mixture was minimal.

(2) Based on the analysis of erosion products from specimens using the semi-immersion method, it was observed that chemical erosion primarily occurred in the immersion zone, while both chemical and physical erosion were present in the alternate wet–dry zone.

(3) Although the chain extender component improved the internal pore structure of the concrete, further research is needed to assess the impact on concrete strength.

(4) According to the evaluation using the 0–1 scoring method, Water Reducer 3 received a score of 20, while Water Reducer $3^{\#}$–1 received a score of 4. Considering these

results comprehensively, the chain extender component exhibited good adaptability to ordinary concrete.

(5) To validate the effectiveness of the 0–1 scoring method, it was applied to evaluate the adaptability of fly ash and slag blended cement concrete. Water Reducer 3 obtained a score of 13, while Water Reducer 3$^{\#}$–1 received a score of 10. Considering these results comprehensively, the chain extender component demonstrated good adaptability to fly ash and slag blended cement concrete.

(6) Overall, this method takes into consideration workability, strength, as well as impermeability, sulfate attack resistance, and alkali–aggregate reactions. It serves as a comprehensive evaluation method for assessing the adaptability of water reducers to concrete. This method can provide a reference for future research on the adaptability of water reducers to concrete.

(7) In order to improve the sulfate corrosion resistance of concrete and to prepare sulfate corrosion resistant concrete, it is necessary to study the influence of other water reducers and admixtures on the sulfate corrosion resistance of concrete and the adaptability between the water reducers and admixtures. In addition, in order to further validate the effectiveness of the evaluation method, this method should be applied to fly ash, slag and silica fume three-admixture concrete and high-performance concrete (HPC). These findings will be the subject of subsequent publications.

Author Contributions: Methodology, B.W. and X.L.; Validation, Q.Z.; Formal analysis, X.M. and Q.Z.; Investigation, L.Z.; Resources, Y.Z. and L.Z.; Data curation, B.W., X.L. and Q.Z.; Writing—original draft, B.W., X.L. and X.M.; Writing—review & editing, B.W., Y.Z. and L.Z. All authors have read and agreed to the published version of the manuscript.

Funding: This research received no external funding.

Institutional Review Board Statement: Not Applicable.

Informed Consent Statement: Not applicable.

Data Availability Statement: Data are contained within the article.

Conflicts of Interest: The authors declare no conflict of interest.

References

1. Wu, B.; Ji, S.; Zhang, A.; Gong, T. Experimental Study on Efflorescence of High Performance Concrete and Design Suggestions for Mixture Ratio. *J. Electr. Power* **2017**, *32*, 504–510.
2. Jiang, J.; Weng, W.; Qiu, J. Study on sulfate corrosion behavior of concrete under simulated groundwater pressure. *J. Hebei Eng. Univ.* **2019**, *36*, 11–15.
3. Qiao, H.; Qiao, G.; Lu, C. Damage degradation model of concrete based on COMSOL under sulfate environment. *J. Huazhong Univ. Sci. Technol.* **2021**, *49*, 119–125.
4. Yan, C.; Cao, Y.; Liu, S.; Wang, X.; Pang, P. Experimental study on salt corrosion resistance of PVA fiber concrete. *Concrete* **2020**, 56–60.
5. Hou, Y. Study on the mechanical and corrosion resistance of hybrid fiber reinforced concrte. *Funct. Mater.* **2020**, *51*, 11116–11120+11213.
6. Zhang, H.; Zhu, Y.; Han, J. Durability of partially-exposed concrete in sulfate saline soil area. *Concrete* **2015**, 4–8.
7. Li, H.; Sun, W.; Zuo, X. Effect of mineral admixtures on sulfate attack resistance of cement-based materials. *Bull. Silic.* **2018**, 1120–1126.
8. Niu, D.; Wang, J.; Ma, R. Sulfate attack test of shotcrete under dry-wet alternation. *China J. Highw. Transp.* **2016**, *29*, 82–89.
9. Wang, H.; Dong, Y.; Sun, X.; Jin, W. Damage mechanism of concrete deteriorated by sulfate attack in wet-dry cycle environment. *J. Zhejiang Univ.* **2012**, *46*, 1255–1261.
10. Yang, Y.; Zhang, Y.; She, W.; Qian, R. Deterioration mechanism of concrete with initial damage exposed to sulfate attack. *J. Build. Mater.* **2017**, *20*, 705–711.
11. Yang, W.; Ye, X.; Li, R.; Yang, J. Effect of Stray Current on Corrosion and Calcium IonCorrosion of Concrete Reinforcement. *Materials* **2022**, *15*, 7287. [CrossRef] [PubMed]
12. Golewski, G.L. The Effect of the Addition of Coal Fly Ash (CFA) on the Control of Water Movement within the Structure of the Concrete. *Materials* **2023**, *16*, 5218. [CrossRef]

13. Zhu, M.; Liu, S.; Ren, Z.; Zhao, S. Experimental study on mineral admixture improving sulfate resistance of high strength concrete. *North China Univ. Water Resour. Hydropower* **2020**, *41*, 67–72.
14. Geng, O.; Sun, Q.; Li, D. Study on inhibition effect of chloride on sulfate corrosion of recycled concrete. *J. Build. Sci. Eng.* **2020**, *37*, 108–116.
15. Wang, M.; Huang, S.; Li, X. Experimental study on polycarboxylic acid series high performance water reducer modified by chain extender. *Concr. Cem. Prod.* **2015**, 1–5.
16. Santhanam, M.; Cohen, M.D.; Olek, J. Sulfate attack research—Whither now? *Cem. Concr. Res.* **2001**, *31*, 845–851. [CrossRef]
17. Santhanam, M. Studies on Sulfate Attack: Mechanisms, Test Methods, and Modeling. Ph.D. Thesis, Purdue University, West Lafayette, IN, USA, 2001.
18. Neville, A. The confused world of sulfate attack on concrete. *Cem. Concr. Res.* **2004**, *34*, 1275–1296. [CrossRef]
19. Schmidt, T.; Lothenbach, B.; Romer, M.; Neuenschwander, J.; Scrivener, K. Physical and microstructural aspects of sulfate attack on ordinary and limestone blended Portland cements. *Cem. Concr. Res.* **2009**, *39*, 1111–1121. [CrossRef]
20. Liu, K.; Mo, L.; Deng, M. Influence of pH on the formation of gypsumin cement materials during sulfate attack. *Adv. Cem. Res.* **2015**, *27*, 487–493. [CrossRef]
21. Bellmann, F.; Moser, B.; Stark, J. Influence of sulfate solution concentration on the formation of gypsum in sulfate resistance test specimen. *Cem. Concr. Res.* **2006**, *36*, 358–363. [CrossRef]
22. Xie, C.; Wang, Q.; Yu, B.; Zhang, R.; Dai, J.; Guo, Y. Analysis of sulfate corrosion resistance of cement-based composite cementitious at different erosion temperatures. *J. Mater. Sci. Eng.* **2020**, *38*, 571–578+584.
23. Zhang, M. Influence of sulfate corrosion on microstructure characteristics of concrete. *Bull. Silic.* **2020**, *39*, 1160–1165.
24. Zhang, X.; Zhang, R.; Ning, G.; Li, H.; Dou, X.; Xiong, Z. Influence of water-cement ratio on sulfate corrosion resistance of concrete. *J. Railw. Sci. Eng.* **2021**, *18*, 1471–1478.
25. Xie, C.; Wang, Q.; Yu, B.; Zhang, R.; Dai, J.; Wang, Y. Experimental study on sulfate attack resistance of nano SiO_2-Slag-Cement composite cementitious material. *J. Mater. Sci. Eng.* **2020**, *38*, 88–93.
26. Tian, S. Experimental Research on Sulfate Corrosion Resistance of Concrete under Dry and Wet Environment. Master's Thesis, Lanzhou Jiaotong University, Lanzhou, China, 2019.
27. Wang, Y. Study on Sulfate Attack Mechanism Andmodifications of Concrete in West of China. Master's Thesis, Lanzhou Jiaotong University, Lanzhou, China, 2016.
28. Grzegorz, L.G. Combined effect of coal fly ash (CFA) and nanosilica (nS) on the strength parameters and microstructural properties of eco-friendly concrete. *Energies* **2023**, *16*, 452.
29. Yang, C. Synergetic Effect of superabsorbent polymer and CaO-based expansive agent on mitigating autogenous shrinkage of UHPC matrix. *Materials* **2023**, *16*, 2814.
30. Wei, H. Compound effects of sodium chloride and gypsum on the compressive strength and sulfate resistance of slag-based geopolymer concrete. *Buildings* **2023**, *13*, 675.
31. Dong, Y.; Ma, Y.; Zhu, J.; Qiu, J. Study on Impermeability of Foamed Concrete Containing Municipal Solid Waste Incineration Powder. *Materials* **2022**, *15*, 5176. [CrossRef]
32. Kang, J. Some basic problems in the research of sulfate corrosion of concrete. *Concrete* **1995**, 7–16.
33. Yang, D.; Zhou, J.; Wang, H.; Liu, R.; Nie, C. Study on the effectiveness of admixtures and mineral admixtures on sulfate resistance of concrete. *Concrete* **2003**, 12–15.
34. He, X.; Ma, B.; Chen, Y. Research and evaluation of mineral admixture on sulfate resistance of concrete. *Concrete* **2003**, 8–11.
35. Ban, K. Inhibition of Admixture on TSA Corrosion of Concrete. Master's Thesis, Chongqing University, Chongqing, China, 2010.
36. Feng, L. Effect of silica fume and water reducer on sulfate corrosion resistance of cement. *J. Southwest Jiaotong Univ.* **1988**, 5–14.
37. Qiao, H. Experimental Study on Sulfate Resistance of High Performance Concrete. Master's Thesis, Lanzhou University of Technology, Lanzhou, China, 2003.
38. Zhang, M.; Guo, C.; Jia, J. Preparation and properties research of high compatibility and multi-branch chain polycarboxylate superplasticizer. *Bull. Silic.* **2019**, *38*, 1274–1277.
39. Wu, W.; Liu, Z.Y.; Ye, Z.; Wang, Y. Synthesis and characterization of phosphonate polycarboxylate superplasticizer with high adaptability. *New Build. Mater.* **2016**, *43*, 39–41+57.
40. Jiang, Z.; Fang, Y.; Guo, Y.; Lin, T. Study on Synthesis and Properties of Vinyl Polyoxyethylene Ether Type Polycarboxylate Superplasticizer. *IOP Conf. Ser. Earth Environ. Sci.* **2020**, *571*, 012135. [CrossRef]
41. Lin, Z. Synthesis and performance study of a highly dispersed HPEG-type polycarboxylate superplasticizer. *J. Phys. Conf. Ser.* **2022**, *2194*, 012028. [CrossRef]
42. Song, Z.; Yao, Y.; Li, T.; Li, X.; Wu, M. Molecular structure design and preparation of slow release polycarboxylic superplasticizer. *J. Build. Mater.* **2017**, *20*, 563–568+574.
43. Zhang, M. Preparation and Properties of low air-entraining and shrinkage-reducing polycarboxylate superplasticizer. *Bull. Silic.* **2017**, *36*, 369–373.
44. Tan, L.; Yan, W.; Zhong, K.; Yang, H.; Tian, M.; Liu, Y. Research on synthesis at room temperature and performance of a high adaptable polycarboxylate superplasticizer. *New Build. Mater.* **2022**, *49*, 136–139.
45. Zhu, X.; Li, X. Synthesis and properties of novel ester monomers and polycarboxylate superplasticizer. *Funct. Mater.* **2022**, *53*, 2182–2186.

46. Lai, H. Preparation and properties of highly adaptive polycarboxylate superplasticizer. *Polym. Notif.* **2022**, 107–112.
47. Guo, F.; Lu, J.; Liu, J.; Qiu, J. Study on the adaptability of polycarboxylate superplasticizer and cement and its mechanism. *New Build. Mater.* **2018**, *45*, 103–107.
48. Tang, X.; Sun, Z.; Liu, Y. Influence of Triethanolamine Grinding Aid on the Compatibility Between Cement and Polycarboxylate Superplasticizer and Its Mechanism. *Mater. Guide* **2018**, *32*, 641–645.
49. Lu, C. Study on the Adaptability of Polycarboxylate Water Reducer in UHPC. Master's Thesis, Hunan University of Technology, Zhuzhou, China, 2020.
50. Tang, H. Corrosion-Resistant Concrete Admixture Study. Master's Thesis, Southwest Jiaotong University, Chengdu, China, 2007.
51. Cai, P. Synthesis and Application of Polycarboxylic Acid Water Reducer. Master's Thesis, Shenyang Jianzhu University, Shenyang, China, 2019.
52. Su, J. Preparation of Polyether Polycarboxylic Acid Water Reducer and Its Adaptability to Cement. Master's Thesis, Shijiazhuang Tiedao University, Shijiazhuang, China, 2019.
53. *GB/T 1345-2005*; The Test Sieving Method for Fineness of Cement. Standards Publishing House: Beijing, China, 2005.
54. *GB/T1346-2011*; Test Methods for Water Consumption, Setting Time, and Soundness of Cement for Standard Consistency. Standards Publishing House: Beijing, China, 2011.
55. *GB/T 1346-2011*; Method of Testing Cements-Determination of Strength. Standards Publishing House: Beijing, China, 2021.
56. *JGJ55-2011*; Specification for Mix Proportion Design of Ordinary Concrete. Construction Industry Press: Beijing, China, 2011.
57. *GB/T50080-2016*; Standard for Test Methods of Performance on Ordinary Fresh Concrete. Construction Industry Press: Beijing, China, 2016.
58. *GB /T 50081-2019*; Standard for Test Methods of Physical and Mechanical Properties of Concrete. Construction Industry Press: Beijing, China, 2019.
59. *GB/T 50082-2009*; Standard for Test Methods of Long-Term Performance and Durability of Ordinary Concrete. Construction Industry Press: Beijing, China, 2009.
60. Peng, X.; Yi, C.; Zhang, Z.; Ouyang, X.; Qiu, X. Effect of polycarboxylate-type water-reducer on dispersion and hydration products of cement. *J. Build. Mater.* **2010**, *13*, 578–583.
61. Hamada, D.; Hamai, T.; Shonaka, M. New superplasticizer providing ultimate workability. *Spec. Publ.* **2006**, *28*, 185–190.
62. Chen, F.; Gao, J.; Qi, B.; Shen, D. Deterioration mechanism of plain and blended cement mortars partially exposed to sulfate attack. *Constr. Build. Mater.* **2017**, *154*, 849–856. [CrossRef]
63. Toyoda, M.; Sakagami, K.; Okano, M.; Okuzono, T.; Toyoda, E. Improved sound absorption performance of three-dimensional MPP space sound absorbers by filling with porous materials. *Appl. Acoust.* **2017**, *116*, 311–316. [CrossRef]
64. El-Hachem, R.; Rozière, E.; Grondin, F.; Loukili, A. Multi-criteria analysis of the mechanism of degradation of Portland cement based mortars exposed to external sulphate attack. *Cem. Concr. Res.* **2012**, *42*, 1327–1335. [CrossRef]
65. Xiong, C.; Jiang, L.; Xu, Y.; Chu, H.; Jin, M.; Zhang, Y. Deterioration of pastes exposed to leaching, external sulfate attack and the dual actions. *Constr. Build. Mater.* **2016**, *116*, 52–62. [CrossRef]